Available online at www.sciencedirect.com
ScienceDirect
Catalysis Today 120 (2007) 358–362
CATALYSIS TODAY
www.elsevier.com/locate/cattod

Synthesis and H_2 uptake of $Cu_2(OH)_3Cl$, $Cu(OH)_2$ and CuO nanocrystal aggregate

S.C. Lee, S.-H. Park, S.M. Lee, J.B. Lee, H.J. Kim *

Energy Nano Material Team, Korea Basic Science Institute, Daejon 305-333, Republic of Korea

Available online 15 November 2006

Abstract

Monodispersed $Cu_2(OH)_3Cl$ nanoplatelets, $Cu(OH)_2$ nanowires, CuO nanoparticles and nanoribbons with a spherical morphology were synthesized using hydrothermal and heat-treatment reactions, and their H_2 storage characteristics were examined. The $Cu_2(OH)_3Cl$ nanoplatelets particles formed immediately after mixing the reactant, which subsequently formed larger uniform spherical particles in the submicron range. This procedure highlights a practical strategy for producing spherical $Cu(OH)_2$ and CuO materials consisting of monodispersed nanocrystals. The spherical aggregates of $Cu_2(OH)_3Cl$ nanoplatelets heat-treated at 473 K could reversibly store up to 2.35 wt.% H_2 at 38 bar and 293 K.

Keywords: Monodispersed nanocrystal; Hydrogen storage; On-board; $Cu_2(OH)_3Cl$; $Cu(OH)_2$; CuO

1. Introduction

Hydrogen has attracted considerable attention as renewable energy source. Efficient conversion technologies, such as fuel cells, are likely to play a major role in the future global energy supply [1,2]. However, the main concern is the efficient storage and transport of this highly flammable gas [3]. The need to store H_2 with satisfactory efficiency to allow its use in stationary and mobile fueling applications has spurred worldwide effort in the development of new materials [4]. Non-carbonaceous nanostructured materials are most promising candidates for H_2 storage on account of their unique chemical, physical and thermodynamic, and transport properties compared with their bulk structures [5].

Monodispersed nanocrystals and their assemblies with an artificial shape and well-defined structures have attracted substantial interest owing to their specific structure and potential applications [6–9]. Since the first controlled synthesis of monodispersed silica spheres in 1968 [10], many methods have been used to produce dense or hollow inorganic hierarchical structures [11–15] using direct or indirect methods such as core-shell approaches using a polymeric bead or other metal dense spheres [16,17], liquid droplet [18], microemulsion [19] and the organization of self-assembled colloidal particles [20,21].

Many copper-based nanostructure materials have been synthesized from copper salt solutions in the presence of urea [22–25], and a number of mineral studies of basic copper(II) chlorides have been undertaken [26–36]. The basic copper(II) chloride of stoichiometric $Cu_2(OH)_3Cl$ is generally known to have four types of crystal structures, atacamite, paratacamite, botallackite and clinoatacamite [26–31].

$Cu(OH)_2$ [37–40] and their basic copper(II) salts such as nitrate [41], carbonate(malachite) [42], and chlorides [43] have been used as a precursor for the preparation of specific nanostructured copper oxide, which is a p-type semiconductor [44] with a narrow band gap (E_g = 1.2 eV). Specific nanostructured copper oxide has been widely exploited as a powerful heterogeneous catalyst [45,46], gas sensors [47,48], lithium ion electrode [49] and field emission emitters [50,51]. However, there have been only a few reports of synthetic $Cu_2(OH)_3Cl$ nanostructures. Jambor et al. [30,31] synthesized atacamite [$CuCl_2{\cdot}3Cu(OH)_2$] microparticles with a bipyramidal shape. Recently, Zhu et al. [43] synthesized α-$Cu_2(OH)_3Cl$ (atacamite) nanoribbons using the bihydrolyzation of $(NH_4)_2CO_3$ as a precursor to make CuO nanoribbons.

H_2 storage with copper based nanomaterials has not been well documented, except for that of materials with a simple cubic $M[M'(CN)_6]$ framework (M = Mn, Fe, Co, Ni, Cu, Zn). These are not copper based nanomaterials but are dehydrated Prussian blue

* Corresponding author. Tel.: +82 42 865 3953; fax: +82 42 865 3419.
E-mail address: hansol@kbsi.re.kr (H.J. Kim).

0920-5861/$ – see front matter
doi:10.1016/j.cattod.2006.09.009

analogues of $Cu_3[Co(CN)_6]_2$ [52]. To our best knowledge, there are no reports of the use of aggregates of monodispersed $Cu_2(OH)_3Cl$ nanoplatelets, $Cu(OH)_2$ nanowires, CuO nanoparticles and nanoribbons with a spherical morphology in reversible hydrogenation and dehydrogenation at much lower temperatures and pressures than with other materials.

2. Experimental

2.1. Materials

Copper(II) chloride dihydrate (99+%), Urea (99%), 1-octanesulfonic acid sodium salt (98%) and sodium hydroxide(99.5%) were purchased from Aldrich and were used without further purification.

2.2. Synthesis of monodispersed $Cu_2(OH)_3Cl$ nanoplatelets, $Cu(OH)_2$ nanowires, CuO nanoparticles and nanoribbons spherical aggregate

Spherical monodispersed $Cu_2(OH)_3Cl$ nanoplatelets, $Cu(OH)_2$ nanowires, CuO nanoparticles and nanoribbons were synthesized via hydrothermal and heat-treatment reactions using $CuCl_2{\cdot}2H_2O$, urea, 1-octanesulphonic acid sodium salt, sodium hydroxide and water system ($CuCl_2{\cdot}2H_2O$:urea:1-octanesulphonic acid sodium salt, molar ratio = 1:2:2).

In a typical synthesis, 2.68 g (0.00157 mol) of $CuCl_2{\cdot}2H_2O$, 1.78 g (0.0296 mol) of urea and 7.38 g (0.0341 mol) of a 1-octanesulfonic acid sodium salt was mixed homogeneously. After thorough mixing, 25 g (1.389 mol) of deionized water were added and stirred vigorously for 1 h. This mixture was placed in a glass bottle in a drying oven at 373 K for 48 h. The hollow sphere types did not appear when molar ratio was changed, and a different kind of alkylsulfonate ($CH_3(CH_2)nSO_3^-Na^+$, n = 3–17; spherical morphology just applies in this case n = 7) was used. Only bipyramidal or other shapes were obtained when the synthetic conditions are altered. Spherical $Cu(OH)_2$ nanowire aggregates (Fig. 1(II)) were produced by stirring the spherical $Cu_2(OH)_3Cl$ nanoplatelets at room temperature with a 1 M NaOH solution for 1 h according to our previous route using anion exchange reactions [53]. The $Cu(OH)_2$ spherical nanowires aggregated into larger spherical CuO nanoparticles (Fig. 1(III)) by heat treatment at 773 K. Spherical CuO nanoribbon aggregates (Fig. 1(IV)) were formed from the spherical $Cu(OH)_2$ nanowires by a hydrothermal reaction at 393 K for 24 h followed by dehydration and further crystallization. All resulting products were filtered, washed with ethanol and deionized water, and finally dried under vacuum at 313 K (Fig. 1).

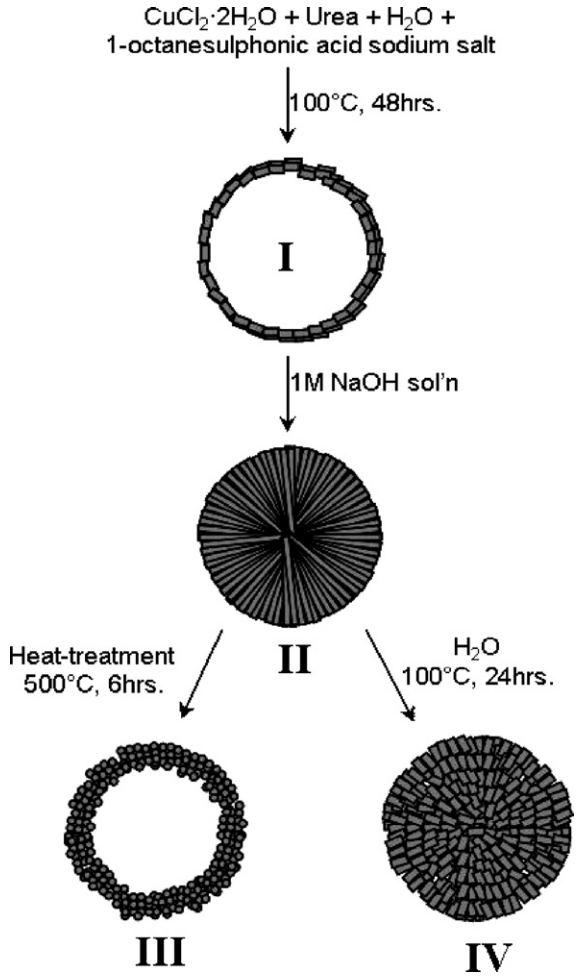

Fig. 1. Schematic illustrations of the formation of $Cu_2(OH)_3Cl$ (I), $Cu(OH)_2$ (II) and CuO nanocrystals (III and IV) presented in this proposed synthesis strategy.

2.3. Characterization

The X-ray powder diffraction (XRD) patterns were obtained on a BRUKER D8 ADVANCE diffractometer using Cu Kα radiation. Scanning electron microscopy and the energy dispersive spectra were obtained on a Leo1455VP SEM and S-4700 field-emission SEM operated at 10 kV. The transmission electron microscope images and selected area electron diffraction (SAED) patterns were obtained on a JEOL 2100F field-emission TEM operated at 200 kV. The samples were prepared by dispersing the particles in absolute ethyl alcohol, dipping a 400 mesh carbon coated copper grids into the suspension, and drying the grids immediately by evaporating the solvent. The H_2 uptake experiments were carried out under a pressure of 38–45 bar at a temperature range of 293–303 K with a SIVERTS volumetric apparatus. The spherical $Cu_2(OH)_3Cl$ nanoplatelet aggregates, typically 0.3 g in weight, were placed into a stainless sample holder that was inserted into the pressure chamber. The chamber was evacuated at 293 K for 5 h under vacuum conditions. After activation at 293 K, high-purity H_2 gas (99.999%, MSGAS Co.) was introduced into the chamber.

3. Results and discussion

3.1. X-ray diffraction patterns

The crystal structures of the as-synthesized samples were first characterization by XRD. Basic copper(II) chloride with a stoichiometry $Cu_2(OH)_3Cl$ is generally known to have four types of crystal structures, atacamite, paratacamite, botallackite

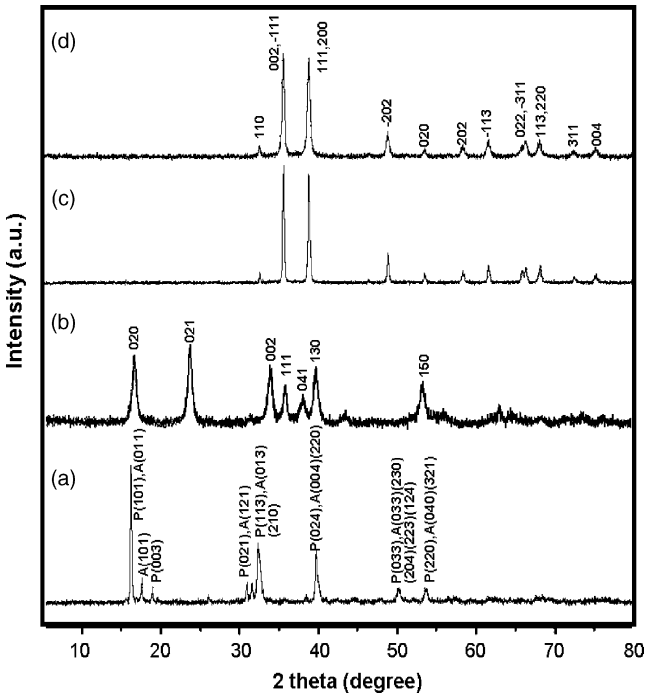

Fig. 2. XRD patterns of the spherical (a) $Cu_2(OH)_3Cl$ nanoplatelets aggregates, (b) $Cu(OH)_2$ nanowires, (c) CuO nanoparticle array and (d) CuO nanoribbons.

and clinoatacamite. From the XRD data shown Fig. 2a, all the reflections of the as-synthesized spherical $Cu_2(OH)_3Cl$ nanoplatelet aggregates could be co-indexed to the orthorhombic atacamite (space group *Pnam*, $a = 6.0479$ Å, $b = 9.1084$ Å, $c = 6.8602$ Å) and rhombohedral paratacamite

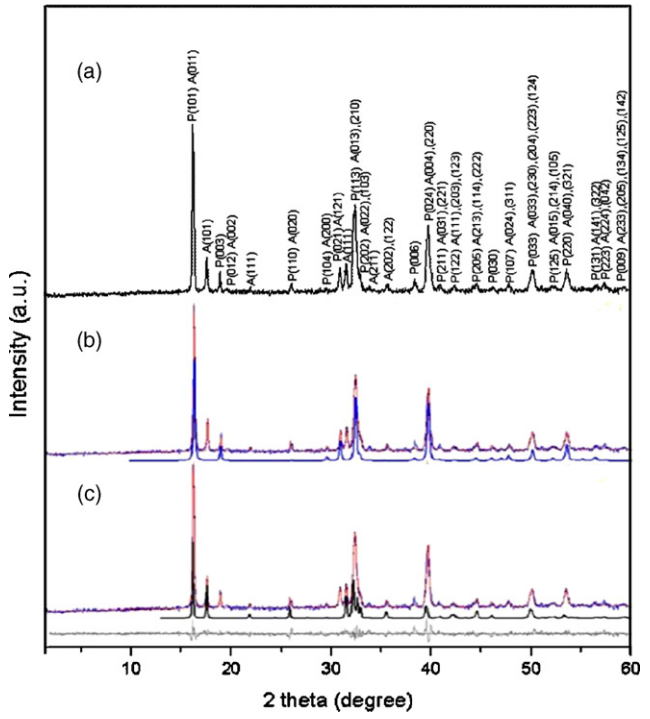

Fig. 3. XRD patterns of the spherical $Cu_2(OH)_3Cl$ nanoplatelet aggregates with a whole indexing (a). X-ray quantitative Rietveld refinement using the TOPAS programs (b and c).

(space group $R\bar{3}m$, $a = 6.8283$ Å and $c = 14.0719$ Å). Fig. 2b shows the XRD patterns of the 1 M NaOH treated samples of $Cu_2(OH)_3Cl$ at 298 K. Spherical $Cu(OH)_2$ nanowires were easily indexed to orthorhombic $Cu(OH)_2$ (space group CMCM, $a = 2.946$ Å, $b = 10.581$ Å, $c = 5.266$ Å). The peaks shown in Fig. 2c and d could be indexed to monoclinic tenorite CuO nanoparticles and the spherical nanoribbons aggregate (space group $C2/c$, $a = 4.6851$ Å, $b = 3.4257$ Å and $c = 5.1311$ Å, $\beta = 99.47°$, JCPDS 45-0937). Fig. 2c shows narrow and sharp peaks, which is in contrast to those shown in Fig. 2d, indicating a large crystal size and better crystallinity than sample shown in Fig. 2d. X-ray quantitative Rietveld refinement using the TOPAS program revealed the as-synthesized spherical $Cu_2(OH)_3Cl$ nanoplatelet aggregates to consist of 67.08 wt.% paratacamite and 32.92 wt.% atacamite phase (Fig. 3).

3.2. Scanning electron microscopy

Fig. 4 shows the general SEM morphology of the as-synthesized nanocrystal aggregates. All the samples shapes

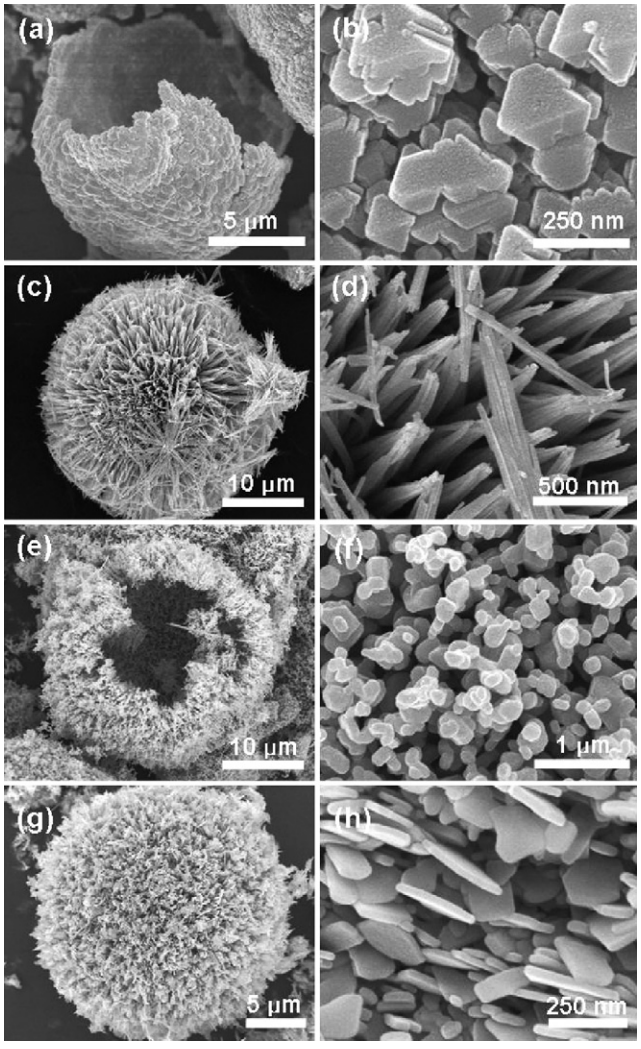

Fig. 4. SEM images of $Cu_2(OH)_3Cl$ nanoplatelets (a and b), $Cu(OH)_2$ nanowires (c and d), CuO nanoparticles (e and f) and spherical nanoribbon aggregate (g and h).

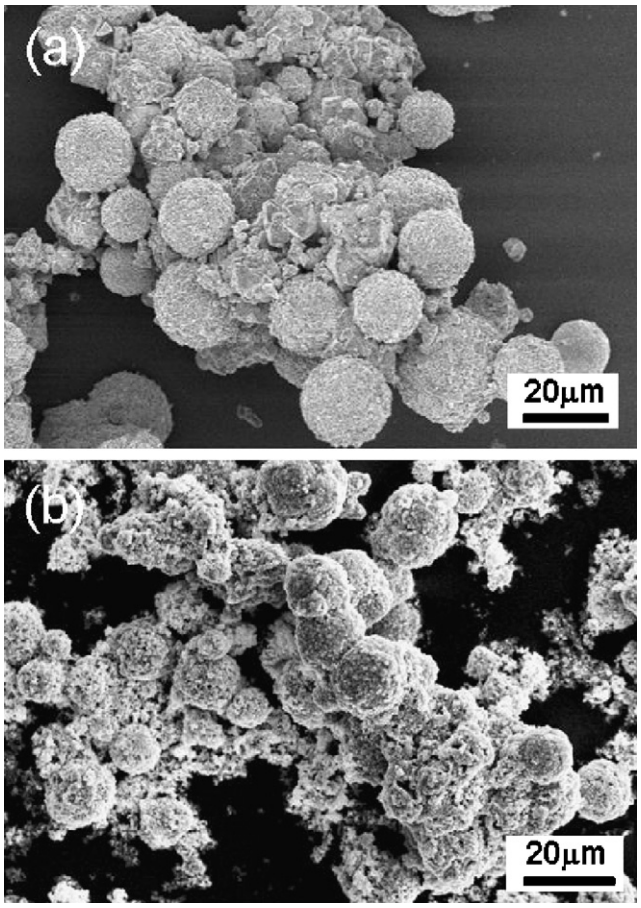

Fig. 5. SEM images of 473 K (a)/773 K (b) heat-treated spherical nanoplatelet aggregates.

exhibited a spherical morphology and consisted of various nanocrystals, such as nanoplatelets, nanowires, nanoparticles and nanoribbons. The hollow spherical aggregate morphologies did not appear when the molar ratio was changed and a different type of alkylsulfonate were used. Only bipyramidal or other shapes were obtained when the synthetic conditions were altered.

$Cu_2(OH)_3Cl$ nanoplatelet particles formed immediately after mixing the reactant, which was followed by larger uniform spherical morphologies in the submicrometer range. This provide a practical strategy for fabricating spherical $Cu(OH)_2$ and CuO materials consisting of monodispersed nanocrystals. No purification process is needed because the sample had good purity and the spherical $Cu_2(OH)_3Cl$ nanoplatelet and CuO nanoparticle aggregate had partially destroyed the hollow interior space (Fig. 4a and e). The spherical nanoplatelet aggregates heat-treated at 473 K/773 K were well preserved (Fig. 5).

3.3. Transmission electron microscopy

The nanosize crystallites were obtained immediately after the reactants had been mixed in the reactor, which then began to aggregate upon aging. Fig. 6 shows the morphology of the nanocrystals and their aggregate. The conversion of

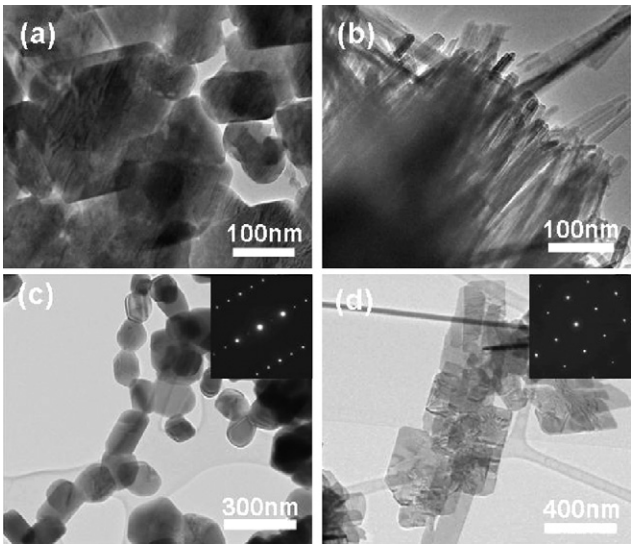

Fig. 6. TEM images of the various monodispersed nanocrystals. (a) $Cu_2(OH)_3Cl$ nanoplatelets, (b) $Cu(OH)_2$ nanowires, (c) CuO nanoparticles array and (d) CuO nanoribbons.

$Cu_2(OH)_3Cl$ nanoplatelets into $Cu(OH)_2$ nanowires, CuO nanoparticles and CuO nanoribbons are also shown. The synthetic spherical $Cu_2(OH)_3Cl$ nanoplatelet aggregates contained pores several tens nanometer in size. The SAED patterns taken of the respective nanoparticles and nanoribbons showed that all the products had single-crystal structures (inset of the Fig. 6c and d).

3.4. Hydrogen sorption property

The spherical $Cu_2(OH)_3Cl$ nanoplatelets aggregates heat-treated at 473 K could reversibly store up to 2.35 wt.% H_2 at 38 bar and 293 K. H_2 saturation was observed after 16 h (Fig. 7). The as-synthesized and samples heat-treated at 773 K could adsorb H_2 up to 0.65 wt.% and 0.41 wt.%, respectively, at 45 bar at 303 K. These H_2 uptake rates might be due to the different structural morphologies. This sample has many merits (high H_2 storage capacity at 38 bar at 293 K) but also some

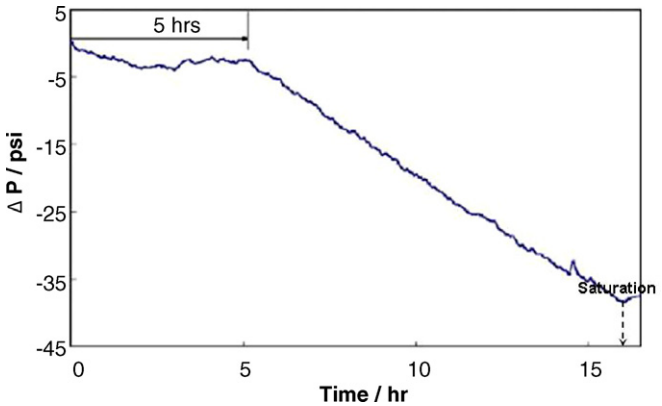

Fig. 7. H_2 uptake in the 473 K heat-treated spherical $Cu_2(OH)_3Cl$ nanoplatelet aggregates under 38 bar at 293 K. After 5 h activation at 293 K, a 2.35 wt.% H_2 uptake capacity could be observed.

demerits (slow H_2 absorption, 16 h). The conversion of the pressure to storage capacity was determined using Redlich–Kwong's equation.

4. Conclusions

Monodispersed $Cu_2(OH)_3Cl$ nanoplatelets, $Cu(OH)_2$ nanowires, CuO nanoparticles and nanoribbons with a spherical morphology were synthesized using hydrothermal and heat-treatment reactions, and their H_2 storage characteristics were examined. This technique is expected to provide a practical strategy for fabricating $Cu(OH)_2$ and CuO materials consisting of monodispersed nanocrystals with a spherical morphology. The advantages of this method lay in the mild reaction conditions used, which allows large-scale production at a low cost. In addition, the empty space of the spherical nanocrystals aggregate would be useful for the preparation of an organic or inorganic domain-filling system. The spherical $Cu_2(OH)_3Cl$ nanoplatelet aggregates heat-treated at 473 K could reversibly store up to 2.35 wt.% H_2 at 38 bar and 293 K. Further investigations of the H_2 capacity of copper nanocrystals are currently underway.

Acknowledgements

This work was performed for Hydrogen Energy R&D center, a 21st Century Frontier R&D Program, funded by the Ministry of Science and Technology of Korea.

References

[1] B.D. McNicol, D.A.J. Rand, K.R. Williams, J. Power Sources 100 (2001) 47.
[2] A.B. Stambouli, E. Traversa, Renewable Sustainable Energy Rev. 6 (2002) 297.
[3] J.M. Ogden, Annu. Rev. Energy Environ. 24 (1999) 227.
[4] L. Schlapbach, A. Züttel, Nature 14 (2001) 353.
[5] A.M. Seayad, D.M. Antonelli, Adv. Mater. 16 (2004) 765.
[6] S.H. Chen, Z.Y. Fan, D.L. Carroll, J. Phys. Chem. B 106 (2002) 10777.
[7] T.D. Ewers, A.K. Sra, B.C. Norris, R.E. Cable, C.H. Cheng, D.F. Shantz, R.E. Schaak, Chem. Mater. 17 (2005) 514.
[8] H.G. Yang, H.C. Zeng, Angew. Chem. Int. Ed. 43 (2004) 5930.
[9] X.J. Yang, Y. Makita, Z.H. Liu, K. Sakane, K. Ooi, Chem. Mater. 16 (2004) 5581.
[10] W. Stober, A. Fink, E.J. Bohn, J. Colloid Interf. Sci. 26 (1968) 62.
[11] Z. Zhong, Y. Yin, B. Gates, Y. Xia, Adv. Mater. 12 (2000) 206.
[12] F. Caruso, Adv. Mater. 13 (2001) 11.
[13] S.W. Kim, M. Kim, W.Y. Lee, T. Hyeon, J. Am. Chem. Soc. 124 (2002) 7642.
[14] Y. Sun, Y. Xia, Science 298 (2002) 2176.
[15] J. Goldberger, R. He, Y. Zhang, S. Lee, H. Yang, J.-J. Choi, P. Yang, Nature 422 (2003) 599.
[16] M.L. Breen, A.D. Donsmore, R.H. Pink, S.Q. Qadro, B.R. Ratna, Langmuir 17 (2001) 903.
[17] K.P. Velikov, A. Van Blaaderen, Langmuir 17 (2001) 4779.
[18] J. Huang, Y. Xie, B. Li, Y. Yin, Y. Qian, S. Zhang, Adv. Mater. 12 (2000) 808.
[19] C.E. Fowler, D. Khushalani, S. Mann, Chem. Commun. (2001) 2028.
[20] B. Liu, H.C. Zeng, J. Am. Chem. Soc. 126 (2004) 16744.
[21] Y. Xu, D. Chen, X. Jiao, J. Phys. Chem. B 109 (2005) 13561.
[22] R.R. Clement, C.J. Serna, M. Ocana, E.J. Matijevic, Crystal Growth 143 (1994) 277.
[23] S.H. Lee, Y.S. Her, E.J. Matijevic, Colloid Interf. Sci. 186 (1997) 93.
[24] E. Matijevic, Chem. Mater. 5 (1993) 412.
[25] S. Kratohvil, E.J. Matijevic, Mater. Res. 6 (1991) 766.
[26] A.F. Wells, Acta Cryst. 2 (1949) 175.
[27] H.R. Oswald, J.R. Guenter, J. Appl. Crystallogr. 4 (1971) 530.
[28] M.E. Fleet, Acta Crystallogr. B 31 (1975) 183.
[29] F.C. Hawthorne, Mineral. Mag. 49 (1985) 87.
[30] J.L. Jambor, J.E. Dutrizac, A.C. Roberts, J.D. Grice, J.T. Szymanski, Can. Mineral. 34 (1996) 61.
[31] J.D. Grace, J.T. Szymanski, J.L. Jambor, Can. Mineral. 34 (1996) 73.
[32] A.M. Pollard, R.G. Thomas, P.A. Williams, Mineral. Mag. 53 (1989) 557.
[33] K.B. Quast, Miner. Eng. 13 (2000) 1647.
[34] M.R. Bisengalieva, I.A. Kiseleva, L.V. Melchakova, L.P. Ogorodova, A.M. Gurevich, J. Chem. Thermodyn. 29 (1997) 345.
[35] S. Weiner, L. Addadi, Science 298 (2002) 375.
[36] H.C. Lichtenegger, T. Schöberl, M.H. bartl, H. Waite, G.D. Stucky, Science 11 (2002) 389.
[37] W.Z. Wang, G.H. Wang, X.S. Wang, R.J. Zhang, Y.K. Liu, C.L. Zheng, Adv. Mater. 14 (2002) 67.
[38] X.G. Wen, W.X. Zhang, S.H. Yang, Z.R. Dai, Z.L. Wang, Nano Lett. 2 (2002) 1397.
[39] X.G. Wen, W.X. Zhang, S.H. Yang, Langmuir 19 (2003) 5898.
[40] W. Zhang, X. Wen, X. Yang, Y. Berta, Z.L. Wang, Adv. Mater. 15 (2003) 822.
[41] C. Henrist, K. Traina, C. Hubert, G. Toussaint, A. Rulmont, R. Cloots, Cryst. Growth 254 (2003) 176.
[42] L. Zhang, J.C. Yu, XuF A.-W., Q. Li, K.W. Kwong, S.-H. Yu, J. Cryst. Growth 266 (2004) 545.
[43] C. Zhu, C. Chen, L. Hao, Y. Hu, Z. Chen, J. Cryst. Growth 263 (2004) 473.
[44] F.P. Koffyberg, F.A. Benko, J. Appl. Phys. 53 (1982) 1173.
[45] J. Ramirez-Ortiz, T. Ogura, J. Medina-Valtierra, S.E. Acota-Ortiz, P. Bosch, J.A. de los Reyes, V.H. Lara, Appl. Surf. Sci. (2001) 174.
[46] J.B. Reitz, E.I. Solomon, J. Am. Chem. Soc. 120 (1998) 11467.
[47] B. Liao, Q. Wei, K.Y. Wang, Y.X. Liu, Sens. Actuators 80 (2001) 208.
[48] T. Ishihara, M. Higuchi, T. Ito, M. Tanigaki, H. Nishiguch, Y. Takita, J. Mater. Chem. 8 (1998) 2037.
[49] X.P. Gao, J.L. Bao, G.L. Pan, H.Y. Zhu, P.X. Huang, F. Wu, D.Y. Song, J. Phys. Chem. B 108 (2004) 5547.
[50] C.T. Hsieh, J.M. Chen, H.H. Lin, H.C. Shin, Appl. Phys. Lett. 83 (2003) 3383.
[51] J. Chen, S. Deng, N. Xu, W. Zhang, X. Wen, S. Yang, Appl. Phys. Lett. 83 (2003) 746.
[52] S.K. Steven, R.L. Jeffrey, J. Am. Chem. Soc. 127 (2005) 6506.
[53] ParkF S.-H., H.J. Kim, J. Am. Chem. Soc. 126 (2004) 14368.